NCTF Control for Friction Compensation of Underactuated Fingers

J. Jalani[1,2] and MK. Ishak[1]
[1] Mechanical Engineering, University of Bristol, Queen's Building University Walk Bristol BS8 1TR UK
Email: jamalj@uthm.edu.my
[2] Department of Technology, Faculty of Electrical and Electronic, University Tun Hussein Onn Malaysia, Batu Pahat Johor Malaysia
Email: memki@bris.ac.uk

***Abstract*—An appropriate control scheme must be used to alleviate nonlinearities and uncertainties for the plant system. However, this is not a trivial task due to the fact that modeling the nonlinearities such as friction and stiction are always inaccurate. For this, adaptive and robust control approaches are preferable. Thus, this paper investigates a new suggested controller scheme namely Nominal Charactersitic Trajectory Following Contoller (NCTF) to mitigate the nonlinearities and/or uncertaintites in particular to counteract the friction of the servo mechanism for the Bristol Elumotion Robot Hand (BERUL). The NCTF control performance will be compared with an adaptive control in simulation. Comparative performance characteristics have shown that the NCTF control has produced lower total control energy than the adaptive control when controlling the tracking and positioning for underactuated fingers.**

***Keywords*—NCTF control, adaptive control and underactuated fingers.**

I. Introduction

Friction can be described as the tangential reaction force between two surfaces in contact. Frictions can be found in all mechanical systems such as servo mechanisms, bearings, transmissions, hydraulic and pneumatic cylinders, valves, brakes and wheels. In many cases friction is always treated as a problem that can deteriorate the performance of the system in particular to achieve high precision system. However, friction is also very important for the control engineer, for example in design of drive systems, high-precision servo mechanisms, robots, pneumatic and hydraulic systems and anti-lock brakes for cars. Moreover, friction is highly nonlinear and may result in steady state errors, limit cycles, and poor performance. Hence, modelling friction is not a trivial and it is always inaccurate. However with the advanced of the computational power such as Matlab, Labview and Maplesim, the accuracy of modelling can be enhanced. The availability of the above mentioned software may improve the quality, economy, and safety of a system. Similarly, grasping an object becomes more challenging if the fingers have the friction and stiction. Joint friction and stiction must be considered in the controller design process. Previous studies by [1], [2], [3] and [4], have shown that friction must be appropriately compensated for accurate motion. BERUL fingers are crucially affected by friction and stiction and therefore, suitable friction compensation approaches are introduced to alleviate such problems. For this, it must be noted that the exact friction model is difficult to obtain in practice. Thus, adaptive and robust control approaches have to be are preferable. Often, robot fingers consist of more degrees of freedom (DOF) than the number of actuators, which are however constrained or interconnected to allow for suitable control. This scenario is called underactuated fingers. The underactuated finger is always difficult to be controlled especially when Cartesian space control is implemented [5]. In order to realize the whole grasping task, first, we have to consider tracking control. Various control techniques have been studied by different groups of researchers to perform tracking control for underactuated systems such as [6], [7] and [8]. The objective of this research is to find out the most suitable controller to counteract the friction and stiction of the underatuated finger. It is anticipated that the chosen controller is able to perform the trajectory tracking and the position control satisfactorily. In the case of the BERUL fingers, for counteracting issues of stiction and friction, we propose two different control schemes namely an adaptive control proposed by [4] and a nominal characteristic trajectory following (NCTF) proposed by [9] and [10]. These two controller are known to be robust towards nonlinearties and uncertainties. This paper is organized as follows. Section II presents the dynamic analysis of the underactuated finger. Section III presents controller design strategies. Section IV discusses the controller performance, followed by the conclusion in section V.

II. Dynamics model of underactuated

Fig. 1 shows the underactuated BERUL hand for which a generic model of each finger needs to be derived for control . The hand has 5 fingers with 16 degrees of freedom and all of the fingers are underactuated.

Figure 1. Underactuated fingers

Presenting a general model of a robot:

© 2012 ACEEE
DOI: 01.IJCSI.03.01. 46

ACEEE

$$M(q)\ddot{q} + V(q,\dot{q})\dot{q} + G(q) = \tau \quad (1)$$

where *M*, *V* and *G* provide mass, velocity and gravity terms respectively. The torque vector τ represents the external torques affecting each joint by the following equations:

$$\theta_2 = 1.0552\theta_1 + 57.7723. \quad (2)$$

$$\theta_3 = 1.3805\theta_2 - 0.1006. \quad (3)$$

Thus, the input torques is constrained by this kinematics relationship, which will be discussed here (see Fig. 2).

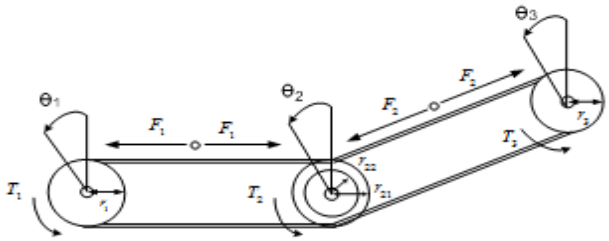

Figure 2. An illustration of a pulley-belt system where the angle, force and torque relationship can be computed from

Having found the kinematics constraints, a dynamic equation has to be derived. Assuming a three degree of freedom system:

$$\begin{bmatrix} M_{11} & M_{12} & M_{13} \\ M_{21} & M_{22} & M_{23} \\ M_{31} & M_{32} & M_{33} \end{bmatrix} \begin{bmatrix} \ddot{\theta}_1 \\ \ddot{\theta}_2 \\ \ddot{\theta}_3 \end{bmatrix} + \begin{bmatrix} VG_1 \\ VG_2 \\ VG_3 \end{bmatrix} = \begin{bmatrix} T_D \\ T_2 \\ T_3 \end{bmatrix} \quad (4)$$

$$\begin{bmatrix} T_1 \\ T_2 \\ T_3 \end{bmatrix} = \begin{bmatrix} T_D - T_{L21} \\ T_{L22} - T_{L31} \\ T_{L32} \end{bmatrix} \quad (5)$$

The terms VG_1, VG_2 and VG_3 represent the lumped expressions of coriolis/centrifugal force and gravity effects. We assume that joint 1 is connected to joint 2 via the pulley-belt system approach (see Fig. 2). The terms T_1, T_2 and T_3 represent the actual torque for each pulley that has been produced by its own driving torque and load torque. Hence $T_1 = T_D - T_{L21}$ is subject to the driving torque T_D and the load torque T_{L21}, due to the torque T_{L22} driving link 2. Similar, the torque $T_2 = T_{L22} - T_{L31}$ has to be discussed where T_{L31} is the load torque, which creates the driving torque T_{L32} for link 3.

$$T_{L21} = r_{21}F_1,\ T_{L22} = r_1F_1 \text{ yields } T_{L22} = \frac{r_1}{r_{21}}T_{L21} \quad (6)$$

$$T_{L31} = r_{22}F_2,\ T_{L32} = r_3F_2 \text{ yields } T_{L32} = \frac{r_3}{r_{22}}T_{L31}. \quad (7)$$

Hence, some computation using equations of (2), (3), (6) and (7) imply the following final equation:

$$\begin{aligned} &(M_{11} + \frac{r_{21}}{r_1}M_{21} + \frac{r_{21}}{r_1}\frac{r_{22}}{r_3}M_{31} \\ &+ \frac{r_1}{r_{21}}M_{12} + M_{22} + \frac{r_{22}}{r_3}M_{32} \\ &+ \frac{r_{22}}{r_3}\frac{r_1}{r_{21}}M_{13} + \frac{r_{22}}{r_3}M_{23} + \frac{r_{22}^2}{r_3^2}M_{33})\ddot{\theta}_1 \\ &+ VG_1 + \frac{r_{21}}{r_1}VG_2 + \frac{r_{21}}{r_1}\frac{r_{22}}{r_3}VG_3 = T_1 \end{aligned} \quad (8)$$

III. Controller design strategies

For controller design, the model

$$m\ddot{q} + f = u \quad (9)$$

is considered, where m is the generalized mass/inertia, f is a lumped expression for the major nonlinearities i.e. gravity, friction and centrifugal/coriolis force.

A. Adaptive Controller

In the adaptive controller, the following equation represents the control error:

$$e = q_d - q \quad (10)$$

with $[q_d(t)\ \dot{q}_d(t)\ \ddot{q}_d(t)]$ being the reference trajectory and its time derivatives. A filtered control error is

$$r = \dot{e} + \lambda e \quad (11)$$

where $\lambda > 0$. Introducing the reference velocity and acceleration signals as

$$\dot{q}_r = \dot{q}_d + \lambda e \quad (12)$$

$$\ddot{q}_r = \ddot{q}_d + \lambda\dot{e}. \quad (13)$$

Consider the controller given by

$$u = \hat{m}\ddot{q}_r + \hat{f} + k_1 r + u_r + k_i\int_0^t r d\tau \quad (14)$$

where $\hat{f}$ is an estimate of the friction force and $\hat{m}$ is an estimate of the mass m. The friction force for control can be modeled as a linearly parameterized nonlinear signal:

$$f = S^T P + \varepsilon \quad (15)$$

where $S = [q\ \delta(\dot{q}),\ sgn(\dot{q}),\ \dot{q},\ \dot{q}|\dot{q}|,\ \sqrt{|\dot{q}|}sgn(\dot{q})]^T \in \Re^L$ are the basis functions used for friction identification. $P \in \Re^L$ is a vector of parameters. The value ε is a small

© 2012 ACEEE
DOI: 01.IJCSI.03.01.46

remaining error. Let $(\hat{*})$ be the estimate of (*) and $(\tilde{*}) = (*) - (\hat{*})$. The closed-loop system is then given by

$$m\dot{r} + k_1 r + u_r + k_i \int_0^t r d\tau = \tilde{m}\ddot{q}_r + \tilde{f} + \varepsilon \qquad (16)$$

where $k_1 > 0$ and a robust control term $u_r = k_2 sgn(r)$ is introduced to compensate for any remaining modeling uncertainty ε. Equation (16) can be further written as

$$m\dot{r} + k_1 r + u_r + k_i \int_0^t r d\tau = d + \varepsilon + \psi^T \tilde{\theta} \qquad (17)$$

where $\psi = [\ddot{q}_r \ S^T]^T$ and $\tilde{\theta} = [\tilde{m} \ \tilde{P}]^T$. The adapting law is

$$\dot{\hat{\theta}} = \Gamma \psi r - \sigma \hat{\theta} \ \ where \ \Gamma^T = \Gamma > 0, \ \sigma \geq 0. \qquad (18)$$

The value σ introduces a forgetting factor, usually resulting in more robust performance. Note that $\dot{\hat{\theta}}$ is responsible for the estimate of $\hat{m}$ and the weights used in the estimate of $\hat{f}$. [4] suggested the following Lyapunov function for closed loop analysis to achieve asymptotic stability for the controller error and bounded stability in the estimates P.

$$V = \frac{1}{2} m r^2 + \frac{1}{2} \tilde{\theta}^T \tilde{\theta} + \frac{1}{2} k_i \left(\int_0^t r d\tau\right)^2 \qquad (19)$$

B. Nominal Characteristic Trajectory Following Controller (NCTF)

The structure of the NCTF control system is shown in Fig. 3.

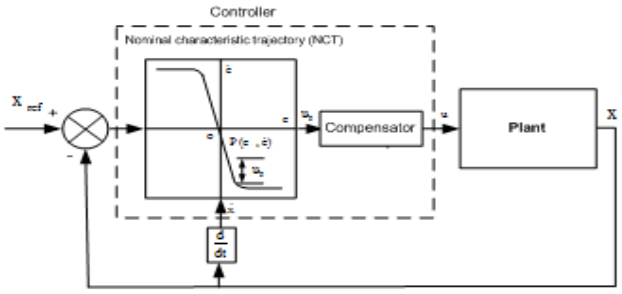

Figure 3. NCTF control system

The NCTF controller consists of a nominal characteristic trajectory (NCT) and a compensator. The NCTF controller works under these two following assumptions:

1. A DC or an AC servomotor is used as an actuator of the object.

2. PTP positioning systems are discussed, so x_{ref} is constant and $\dot{x}_{ref} \equiv 0$.

Here, the objective of the NCTF controller is to make the object motion follow the NCT and end at the origin of the phase plane $(e, \dot{e})$.

Fig. 4 shows an example of object motion controlled by the NCTF controller. The motion comprises of two phases. The first phase is the reaching phase and the other phase is the following phase. In the reaching phase, the compensator forces the object motion to reach the NCT as fast as possible. Then, in the following phase, the compensator controls the object motion to follow the NCT and end at the origin. The object motion stops at the origin, which represents the end of the positioning motion. Thus, in the NCTF control system, the NCT governs the positioning response performance.

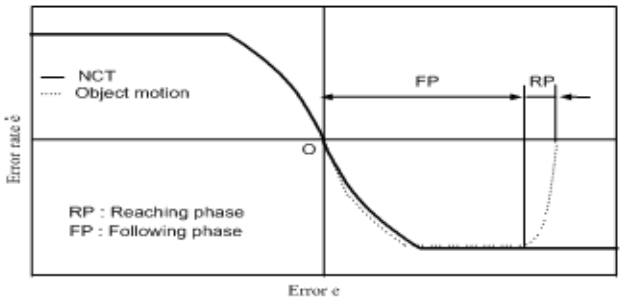

Figure 4. NCT and object motion

The NCTF controller is designed based on a simple open-loop experiment of the object as stated below:

1. The open-loop-drive the object with stepwise inputs and measure the displacement and velocity responses of the object. Fig. 5 shows the velocity and displacement responses due to the stepwise inputs. In this section, the rated input to the actuator u_r is used as height of the stepwise inputs.
2. Construct the NCT using the object responses. The velocity and displacement responses are used to determine the NCT. Since the main objective of PTP system is to stop an object at certain position, a deceleration process (curve in area A of Fig. 5(a)) is used. Variable h in Fig. 5 is the maximum motion velocity. From the curve in area A and h in Fig. 5(a), the NCT in Fig. 5(b) is determined. Since the NCT is constructed based on the actual responses of the object, the NCT includes nonlinearity effects such as friction and saturation.
3. Design the compensator based on the NCT information. Here the following PI compensator is adopted due to its simplicity:

$$u = K_p u_p + K_i \int u_p dt \qquad (20)$$

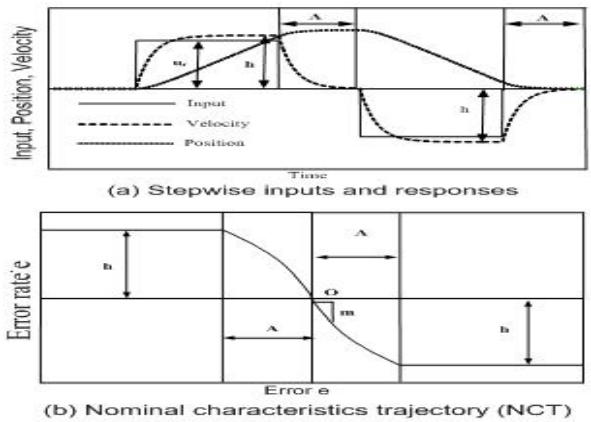

Figure 5. NCT determination

© 2012 ACEEE
DOI: 01.IJCSI.03.01.46

ACEEE

where K_p and K_i are proportional and integral gains respectively. Using the PI compensator parameters K_p and K_i, and the NCT characteristic near the origin (see Fig. 5(b)), the transfer function of the closed-loop positioning system controlled by the NCTF controller can be approximated as follows:

$$\frac{X(s)}{X_{ref}(s)} = G(s) = G_1(s)G_2(s) \tag{21}$$

where

$$G_1(s) = \frac{\alpha}{s+\alpha} \tag{22}$$

$$G_2(s) = \frac{2\zeta\omega_n + \omega_n^2}{s^2 + 2\zeta\omega_n + \omega_n^2} \tag{23}$$

$$K_p = \frac{2\zeta\omega_n}{K\alpha}, \quad K_i = \frac{\omega_n^2}{K\alpha} \tag{24}$$

where α is the simplified object parameter, ζ is the damping ratio and ω_n is the natural frequency. When ζ and ω_n are large enough, G(s) becomes nearly equal to $G_1(s)$, which represent the condition when the object motion follows the NCT as the objective of the NCTF control system. Moreover, large ζ and ω_n also make the closed-loop system robust to friction or inertia variation of the object in continuous systems [9]. Finally, by using ζ and ω_n as design parameters the PI compensator parameters are designed as follows:

$$K_p = \frac{2\zeta\omega_n u_r}{mh}, \quad K_i = \frac{\omega_n^2 u_r}{mh} \tag{25}$$

III. SIMULATION

To show the effectiveness of the proposed control algorithm, we have carried out the simulation by using dynamic of the system as in equation (9). In particular the frictional force of f in equation (9) is defined as follows:

$$f = \sigma_0 z + \sigma_1 \frac{dz}{dt} + f_v \dot{x} \tag{26}$$

$$\frac{dz}{dt} = \dot{x} - \frac{|\dot{x}|}{g(\dot{x})} z \tag{27}$$

The frictional force f considered here is represented by the Z model which captures most friction behaviours, and the factors in the model are chosen as $x_s = 0.001$, $\sigma_0 = 100000$, $\sigma_1 = \sqrt{100000}$, $f_v = 0.4$. Moreover, a filtered squarewave demand signal which has a frequency of (0.2 Hz), amplitude of (0.7 rad), the sampling time of (1 ms) is used. For the demand filter, a second order filter ($K_i = \frac{50}{s^2 + 20s + 50}$) is used. The performance of the adaptive and NCTF controllers are shown in Fig. 6 and Fig. 7 respectively. The selection of the controller gains is shown in Table I for adaptive and NCTF controllers.

TABLE I
ADAPTIVE AND NCTF GAIN SELECTION

Controllers	k_1	k_i	k_2	Γ	σ	k_p
Adaptive	80	10	1	1000	1	
NCTF	-	15	-	-	-	50

To compare the results, a quantitative measure of performance as indicated by [11] and [12] is computed as follows:

$$Normalized\ Error = \sum_{i=1}^{N_s} | y_{di} - y_i | / N_s \tag{28}$$

while we also consider

$$Total\ Control\ Signal\ Energy = \sum_{i=1}^{N_s} | u_i |^2 / N_s \tag{29}$$

where y_{di} is the demand signals, y_i is the output signal, N_s is the number of samples and u_i is the control signal. Generally, the results show that adaptive and NCTF follow a required trajectory satisfactorily. The details of the error signal and total control energy that have been produced by each controller can be referred to Table 2. It is noted that the NCTF has used the lowest total control energy when the signal error is similar. The amount of total control energy has been produced by adaptive controller is almost 2 times than the NCTF controller.

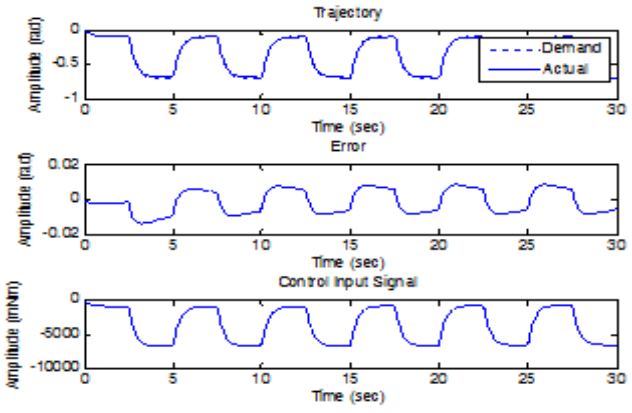

Figure 6. Performance of NCTF control

© 2012 ACEEE
DOI: 01.IJCSI.03.01.46

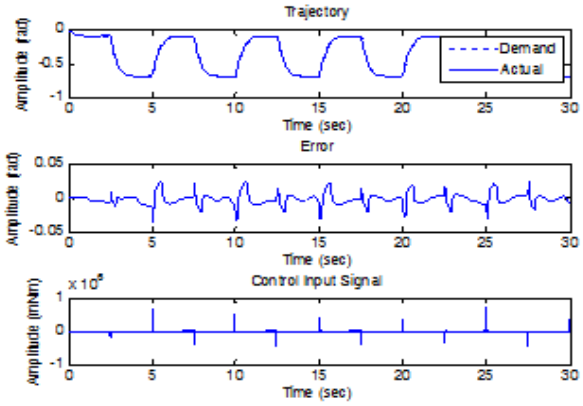

Figure 7. Performance of adaptive control

TABLE II. NORMALIZED ERROR AND TOTAL CONTROL ENERGY USED FOR ADAPTIVE AND NCTF

Controllers	Normalized Error (rad)	Total Control Energy (mNm)
Adaptive	0.0065	6.8751e+003
NCTF	0.0065	3.7407e+003

V Conclusions

In this paper, the NCTF control scheme has been proposed to achive better tracking and positioning controls in simulation. The results show that the NCTF has produced lower total signal energy as compared to the adaptive control. In particular, the NCTF is the most suitable candidate to counteract the friction and stiction for the servo mechanism of the BERUL fingers.

Acknowledgment

The CHRIS (Cooperative Human Robot Interaction Systems) project is funded by the European Commission's Seventh Framework Programme (FP7) and will run from 2008-2012. The research is also partially funded by the Malaysian Government.

References

[1] C. C. de Wit, K. Astrom, and K. Braun, "Adaptive friction compensation in dc-motor drives," *IEEE Journal of Robotics and Automation*, vol. 3, no. 6, pp. 681–685, December 1987.

[2] C. C. de Wit, H. Olsson, K. Astrom, and P. Lischinsky, "Dynamic friction models and control design," *American Control Conference*, pp. 1920–1926, June 1993.

[3] C. C. de Wit and S. Ge, "Adaptive friction compensation for systems with generalized velocity/position friction dependency," *Proceedings of the 36th IEEE Conference on Decision and Control*, vol. 3, pp. 2465–2470, Dec 1997.

[4] S. Ge, T. Lee, and S. Ren, "Adaptive friction compensation of servo mechanisms," *International Journal of Systems Science*, vol. 32, no. 4, pp. 523–532, 2001.

[5] J. Jalani, G. Herrmann, & C.R. Melhuish, *Robust Active Compliance Control for Practical Grasping of a Cylindrical Object via a Multifingered Robot Hand*, 5th IEEE International Conference on Robotics, Automation and Mechatronics (RAM), Qingdao, 2011.

[6] H. Arai, K. Tanie, and N. Shiroma, "Feedback control of a 3-dof planar underactuated manipulator," *IEEE International Conference on Robotics and Automation*, vol. 1, pp. 703–709, Apr 1997.

[7] K. Kobayashi and T. Yoshikawa, "Controllability of Under-Actuated Planar Manipulators with One Unactuated Joint," *The International Journal of Robotics Research*, vol. 21, no. 5-6, pp. 555–561, 2002.

[8] A. Mahindrikar, S. Rao, and R. Banavar, "Point-to-point control of a 2r planar horizontal underactuated manipulator," *Mechanism and Machine Theory*, vol. 41, no. 7, pp. 838–844, July 2006.

[9] Wahyudi, Sato K. and Shimokohbe A.; Characteristics of Practical Control for Point-to-point Positioning Systems: Effect of design parameters and actuator saturation, Precision Engineering, Vol. 27, No. 2, 2003, pp. 157-169.

[10] **Wahyudi,** Jamaludin Jalani, Riza Muhida and Momoh Jimoh Emiyoka Salami, 2007, Control Strategy for Automatic Gantry Crane Systems: A Practical and Intelligent Approach, International Journal of Advanced Robotic Systems,4(40, pp. 447-456.

[11] D. J. S.G. Goodhart, K.J. Burnham, "Self-tuning control of non-linear plant - a bilinear approach," *Transactions of the Institute of Measurement and Control*, vol. 14, no. 05, pp. 227–232,1992.

[12] C. Edwards and S. Spurgeon, "Robust nonlinear control of heating plant," *IEEE Proceedings on Control Theory and Applications*, vol. 141, no. 4, pp. 227–234, Jul 1994.

© 2012 ACEEE
DOI: 01.IJCSI.03.01. 46